



Transferosomes stabilized hydrogel incorporated rhodomertone-rich extract from *Rhodomyrtus tomentosa* leaf fortified with phosphatidylcholine for the management of skin and soft-tissue infections

Julalak Chorachoo Ontong · Sudarshan Singh · Thanyaluck Siriyong · Supayang P. Voravuthikunchai

Received: 22 May 2023 / Revised: 13 October 2023 / Accepted: 10 November 2023 / Published online: 27 December 2023
© The Author(s), under exclusive licence to Springer Nature B.V. 2023

Abstract *Rhodomyrtus tomentosa* leaf (RT)-incorporated transferosomes were developed with lecithin and cholesterol blends with edge activators at different ratios. RT-transferosomes were characterized and employed in transferosomal gel formulations for the management of skin and soft-tissue infections. The optimized formulation entrapped up to $81.90 \pm 0.31\%$ of RT with spherical vesicles (405.3 ± 2.0 nm),

polydispersity index value of 0.16 ± 0.08 , and zeta potential of -61.62 ± 0.86 mV. Total phenolic and flavonoid contents of RT-transferosomes were 15.65 ± 0.04 μg GAE/g extract and 43.13 ± 0.91 μg QE/g extract, respectively. RT-transferosomes demonstrated minimum inhibitory and minimum bactericidal concentrations at 8–256 and 64–1024 $\mu\text{g}/\text{mL}$, respectively. Free radical scavenging assay showed RT-transferosomes with high scavenging activity against DPPH and ABTS radicals. Moreover, RT-transferosomes demonstrated moderate activity against mushroom tyrosinase, with IC₅₀ values of 245.32 ± 1.32 $\mu\text{g}/\text{mL}$. The biocompatibility results against L929 fibroblast and Vero cells demonstrated IC₅₀ at 7.05 ± 0.17 and 4.73 ± 0.13 $\mu\text{g}/\text{mL}$, respectively. In addition, nitric oxide production significantly decreased by 6.78–88.25% following the treatment with 31.2–500 ng/mL RT-transferosomes ($p < 0.001$). Furthermore, the freeze–thaw stability study displayed no significant change in stability in the sedimentation and pH of gel fortified with RT-transferosomes. The results suggested that RT-transferosome formulation can be effectively employed as natural biomedicines for scar prevention and the management of skin soft-tissue infections.

Supplementary Information The online version contains supplementary material available at <https://doi.org/10.1007/s10529-023-03452-1>.

J. C. Ontong (✉)
Cosmetic Technology and Dietary Supplement Products Program, Faculty of Agro and Bio Industry, Thaksin University, Ban Pa Phayom 93210, Phatthalung, Thailand
e-mail: julalak.o@tsu.ac.th

J. C. Ontong · T. Siriyong · S. P. Voravuthikunchai
Center of Antimicrobial Biomaterial Innovation-Southeast Asia, Faculty of Science, Prince of Songkla University, Hat Yai 90112, Songkhla, Thailand

S. Singh
Department of Pharmaceutical Sciences, Faculty of Pharmacy, Chiang Mai University, Chiang Mai 50200, Thailand

S. Singh
Office of Research Administration, Chiang Mai University, Chiang Mai 50200, Thailand

T. Siriyong
Faculty of Traditional Thai Medicine, Prince of Songkla University, Hat Yai 90112, Songkhla, Thailand

Keywords Antibacterial antioxidant · Anti-inflammatory · Rhodomertone · *Rhodomyrtus tomentosa* · Transferosomes

Introduction

Skin and soft-tissue infections (SSTIs) cover various illnesses, including general and complex infections. SSTIs are often mild to severe moderately, including microbial invasion of the skin and surface and underlying soft tissues, and require various therapeutic agents for therapy (Stevens et al. 2005). An etiologic diagnosis of cellulitis is often challenging for patients with mild signs and symptoms of illness. Most SSTIs are caused by *Staphylococcus aureus* and *Streptococci*, which secrete extracellular polymeric substances, which minimizes therapeutic drug activities and enhances colonization due to polysaccharides intercellular adhesion (Kwiecinski et al. 2015). The formation of staphylococci biofilm, particularly in dermal wound infections and skin abscesses, usually increases the severity and chances of bloodstream infection (Cupane et al. 2012). SSTIs incidents have grown recently due to the aging of general populations, an increase in the number of critically sick patients, an increase in the number of immunocompromised patients, and the emergence of resistant pathogens. Several studies indicated the severity of antibiotics failure against patients infected with SSTIs, resulting in increases morbidity and mortality with a significant increase in hospitalization costs.

Due to the increasing resistance of *S. aureus* and MSRA against major antibiotics, skin infections are increasingly difficult to treat. Several studies indicated that phenolic-rich extracts, mainly flavonoids and acylphloroglucinol, possess a wide range of biological applications, including antioxidant, anti-inflammatory, and antimicrobial, and can be an effective alternative in management of SSTIs (Xavier-Santos et al. 2022; Nwabor et al. 2021a, b). Recently rhodomertone, an acylphloroglucinol derivative compound extracted from *Rhodomyrtus tomentosa* (family Myrtaceae) native to Southern and Southeastern Asia reported as a novel antibiotic. It is extensively used in Thai traditional medicine for the treatment of diarrhea (Lavanya et al. 2012), dysentery (Lavanya et al. 2012), gynecopathy (Voravuthikunchai et al. 2010), hemorrhage (Geetha et al. 2010), urinary tract infections (Voravuthikunchai et al. 2010), antiseptic wash for wounds (Geetha et al. 2010), and in the treatment of inflammatory acne lesions (Wunnoo et al. 2021). Rhodomertone has been evidenced to possess antipressant and anti-proliferative properties, affirming

its use for various infectious complications (Ozioma et al. 2022). Moreover, rhodomertone has been reported to preferentially down-regulate transcripts involved in epidermal responses, myeloid leukocyte chemotaxis, and inflammatory responses (Chorachoo et al. 2018). In addition, the excellent antibacterial activities of rhodomertone against Gram-positive pathogenic bacteria of medical importance with safety and efficacy make it a potential candidate for the management of SSTIs (Mordmuang et al. 2021).

Noninvasive self-administration of vesicular drug delivery systems gained much interest recently due to their several advantages against conventional drug delivery systems. Fortification of phytoconstituents using phosphatidylcholine (Patel et al. 2009; Kapoor et al. 2023; Popat et al. 2023) and pure rhodomertone (Chorachoo et al. 2013) within vesicles demonstrated excellent improvement in its efficacy. Therefore, the present study reports the extraction of rhodomertone-rich extract from *Rhodomyrtus tomentosa* leaf and incorporation within vesicular drug delivery transferosomes. Phosphatidylcholine fortified rhodomertone-rich extract from *Rhodomyrtus tomentosa* leaf transferosomes was evaluated for antibacterial, antioxidant, anti-melanogenesis, and anti-inflammatory activity. Further, the transferosomes incorporated rhodomertone-rich extract was stabilized with hydrogel and tested for structural compatibility, biological efficacy, and cytocompatibility against human keratinocyte skin cells. Furthermore, the optimized vesicle formulation was tested by the freeze–thaw to ensure the stability of the formulations (Fig. 1).

Materials and methods

Materials

Purified rhodomertone (standard marker) was obtained from the Natural Product Research Center of Excellence, Prince of Songkla University. Acetonitrile (HPLC grade, 75-05-8), 85% orthophosphoric acid (analytical grade, 7664-38-2), and ethanol (AR grade, 64-17-5) were procured from Labscan Asia (Bangkok, Thailand). L- α -phosphatidylcholine (Mw. 776 g/mol), cholesterol (Mw. 386.5 g/mol), triethanolamine (Mw. 149.188 g/mol), tween 20 (density: 1.1 g/cm³), tween 80 (density: 1.06 g/cm³), span 20 (density: 1.05 g/cm³), span 80 (density: 0.98 g/cm³),

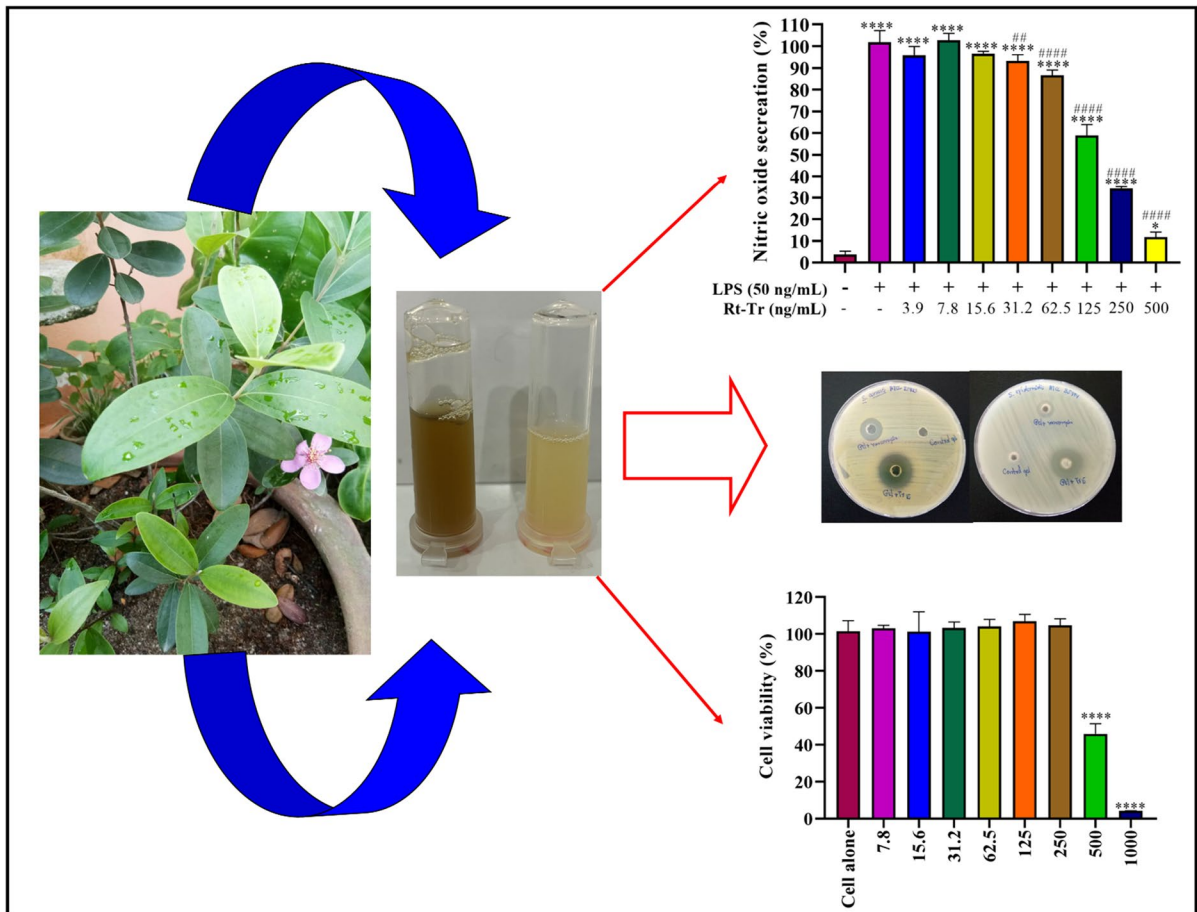


Fig. 1 Graphical illustration of phosphatidylcholine fortified rhodomirtone-rich extract from *Rhodomirtus tomentosa* leaf transferosomes

sodium deoxycholate (Mw. 414.6 g/mol), dimethyl sulfoxide (DMSO: density: 1.1 g/cm³), glycerol (density: 1.26 g/cm³), 2,2-azino-bis (3-ethylbenzothiazoline-6-sulfuric acid) (ABTS⁺: Mw. 548.68 g/mol), L-dopa (Mw. 197.18 g/mol), tyrosinase enzyme from mushroom (1000 U/mg), 2,2-diphenyl-1-picrylhydrazyl (DPPH: Mw. 394.32 g/mol), 3-(4,5-dimethylthiazole-2-yl)-2,5-diphenyl-tetrazolium bromide (MTT), 2,4,6-tri(2-pyridyl)-s-triazine (TPTZ; Mw. 312.3 g/mol), Folin-Ciocalteu (density: 1.24 g/cm³), gallic acid (Mw. 170.12 g/mol), L-ascorbic acid (Mw. 176.12 g/mol), potassium persulfate (Mw. 270.33 g/mol), sodium acetate (Mw. 82.03 g/mol), ferric chloride hexahydrate (Mw. 270.29 g/mol), sodium carbonate (Mw. 105.98 g/mol), aluminum dichloride (Mw. 97.88 g/mol), sodium hydroxide (Mw. 39.99 g/mol), gallic acid (GAE; Mw. 170.12 g/mol), quercetin (QE;

Mw. 302.236 g/mol), sulfanilamide (Mw. 172.202 g/mol), and n-1-naphthylendiamine dihydrochloride (Mw. 259.17 g/mol) were purchased from Sigma-Aldrich, Darmstadt, Germany. Carbopol ultrez-21 was purchased from Lubrizol, Ohio, USA. Bacteriological media, including Mueller Hinton broth (MHB), tryptic soy agar, and tryptic soy broth (TSB) were purchased from Difco (Port de Claix, France). Fetal bovine serum (FBS) was purchased from Biochrom Ltd (Berlin, Germany). Dulbecco's Modified Eagle's (DMEM) was purchased from Cytiva Hyclone, Utah, USA. Penicillin/streptomycin (5000 U/mL), 2 mM stable L-glutamine, and trypsin were purchased from Gibco, Thermo Fisher Scientific, Inc (MA, USA). Bacteria, including *Staphylococcus aureus* ATCC 25923 and *Staphylococcus epidermidis* ATCC 12228, were obtained from a culture collection

laboratory. Murine mouse fibroblast cell line (L929), African green monkey epithelial kidney cell (Vero), mouse macrophage cells (RAW 264.7), and human keratinocyte cells (HaCaT) were procured from CLS Cell Lines Service GmbH (Eppelheim, Germany).

Collection of leaf and extraction of rhodomyltone-rich extract

Rhodomyrtus tomentosa leaves were collected from the Singha-Nakorn District, Songkhla Province, Thailand, in February 2021. The voucher specimen (NPRCoE 201701) is identified by Mr. Jarensak Sea Wai. It has been deposited in the herbarium of the Department of Biology, Faculty of Science, Prince of Songkla University, Thailand. The leaves are washed with tap water and dried in a hot air oven (Memmert GmbH+Co. KG, Schwabach, Germany) at 60 °C for 24 h. The dried leaves are pulverized into powders using an electric blender (Yongkang Tianqui Shengshi Industry and Trade Co. Ltd., Yongkang, Zhejiang, China) and extracted by maceration using ethanol (95% v/v).

Fabrication of rhodomyltone-rich extract fortified transferosome

Vesicle entrapped RT-Tr was prepared by thin-film hydration techniques, as reported (Mordmuang et al. 2015; Wunoo et al. 2021; Chittasupho et al. 2023). A blend of hydroalcoholic stock solution of L- α -phosphatidylcholine and cholesterol containing rhodomyltone-rich extract was prepared with different edge activators such as Tween 80, Tween 20, Span 80, Span 20, and sodium deoxycholate to formulate stable transferosomes as presented in Table S1. The composition of optimized formulations is shown in Table 1. The oil and aqueous phase was partitioned using sonication (Bandelin sonorex digitec, Berlin, Germany) at 60 °C for 30 min until homogeneity. Then, the absolute ethanol was evaporated using a rotary evaporator (Hei-Var-ML, Schwabach, Germany) to form a thin-layer lipid film. The thin-layer lipid film was hydrated with an aqueous phase (10 mL), followed by shaking (WS-500, Beijing, China) (5 min). Finally, the suspension was sonicated at 60 °C for 30 min to obtain uniform shape vesicle entrapped with or without rhodomyltone-rich extract transferosome. Furthermore, the transferosomes were

Table 1 The composition of optimized transferosome formulations

| Formulation code | Lipid phase (w/v) | | Surfactant SDC | RT (w/w) | Aqueous phase (v/v) |
|------------------|-------------------|-------|----------------|----------|---------------------|
| | SPC | CHOL | | | |
| RT-Tr5 | 0.74 | 0.092 | 0.1 | 0.5 | Water |
| RT-Tr10 | 0.74 | 0.092 | 0.2 | 0.5 | Water |
| RT-Tr15 | 0.74 | 0.092 | 1 | 0.5 | Water |

SPC L- α -phosphatidylcholine from soybean, CHOL cholesterol, SDC sodium deoxycholate, RT rhodomyltone-rich extract from *Rhodomyrtus tomentosa* leaf

quantified for color using CIE L* a* b* color space instrument (ColorFlex, USA) with calibration by the manufacturer's standard white plate as reported (Singh et al. 2022a, b). The L* value measures the lightness of the sample, a* indicates the red versus green in the sample, and b* measures the yellow versus blue in the sample. The parameters L*, a*, and b* were used to calculate Chroma, Hue angle, ΔE (total color change) and browning index (BI).

Vesicle sizes, zeta potential, and entrapment efficiency of rhodomyltone transferosome

Vesicle size and zeta potential were quantified by dynamic light scattering (DLS) and electrophoretic light scattering techniques using Malvern Zetasizer (Malvern Instruments Ltd., Malvern, UK) as reported (Nagime et al. 2023). The entrapment efficacy was quantified using UFLC Shimadzu HPLC system equipped with an SPD-M20A photodiode-array detector, SIL-20A HT auto-sampler (Shimadzu Corp. Kyoto, Japan). Briefly, the measured volume (1 mL) of vesicles entrapped RT-Tr was centrifuged using ultracentrifuge (Hettich zentrifugen MIKRO 220R, Tuttlingen, Germany) at 40,000 rpm for 30 min, and the supernatant diluted with methanol. The transferosome samples were filtered by Phree™ Phospholipid Removal (Phenomenex, CA, USA) to remove impurities and injected in HPLC with appropriate dilutions. Rhodomyltone separation was carried out on a C18 column (Kinetex 5u EVO C18 100A 250×4.6 mm, Phenomenex, CA, USA) using a mobile phase consisting of acetonitrile in water (85:15, v/v) at a flow rate of 1 mL/min with a detection wavelength of 254 nm using PDA detector. The quantification of

rhodomyrtonone was calculated from the rhodomyrtonone standard curve ($y = 1.96x + 7.15$; $r = 0.999$).

Antimicrobial activity, antioxidant efficacy, and quantitative phytoconstituents analysis

Gram-positive *S. aureus* ATCC 25923 and *S. epidermidis* ATCC 12228 were cultured on tryptic soy agar at 37 °C for 18 h and stored at – 80 °C in tryptic soy broth containing 20% glycerol. The microdilution method evaluated the antibacterial activity of optimized RT-Tr against reference strains according to Clinical and Laboratory Standardization Institute guidelines (CLSI 2016; Singh et al. 2023a). In brief, two-fold dilutions of transferosome vesicle entrapped RT (8–1024 µg/mL) were treated with diluted bacterial suspension (10^8 CFU/mL) and incubated for 18 h at 37 °C. The lowest concentration that completely inhibited the bacteria growth was recorded as the MIC (µg/mL). The MBC was determined using the spot plate technique by seeding 10 µL aliquots from wells without growth on TSA. The radical scavenging efficacy of RT-Tr was evaluated using DPPH and ABTS⁺ radical scavenging assay, as reported previously (Singh et al. 2022a, b; Auberon et al. 2023). The total phenolic (TPC) and flavonoid contents (TFC) within RT-Tr were determined using Folin-Ciocalteu and aluminum chloride assays as previously reported (Nwabor et al. 2020; Lei et al. 2023) and were expressed in milligram GAE equivalent per milligram of extract and milligram QE equivalent per milligram of extract.

Mushroom tyrosinase inhibition assay

As reported previously, the mushroom tyrosinase inhibition efficacy of optimized RT-Tr was determined by DOPA-chrome method (Singh et al. 2023b). Concisely, 685 µL of phosphate buffer (0.05 M, pH 6.5), 15 µL of mushroom tyrosinase (2500 U/mL), 200 µL of transferosome solution in the concentration range of 16–2048 µg/mL, and 100 µL of 5 mM-L-DOPA were transferred to the 2000 µL microcentrifuge. After addition L-DOPA, the reaction was immediately monitored at 492 nm using microplate reader (Biohit 830, Biohit, Helsinki, Finland) for dopachrome formation in the reaction mixture. L-ascorbic acid was used as a positive control. Each measurement was made in triplicate.

Cytocompatibility of transferosome

Cytotoxicity of optimized RT-Tr against the murine fibroblast cell line (L929), African green monkey epithelial kidney cell (Vero), and macrophage (RAW 264.7) cell was evaluated as reported (Chorachoo et al. 2016). The cells were cultured in high glucose Dulbecco's Modified Eagle Medium (DMEM) supplemented with 10% fetal bovine serum and 100 µg/mL streptomycin and, 100 µg/mL penicillin solution. Approximately 1×10^4 cells/well were seeded in 96-well plates and incubated at 37 °C in an incubator humidified with 5% CO₂ at 37 °C. After 24 h incubation, the spent medium was replaced with fresh DMEM medium. The RT-Tr was diluted two-fold in the wells containing DMEM to yield a final concentration of 1–1000 µg/mL for L929 and Vero cells, while RAW 264.7 was treated with a concentration of 7.8 – 1000 ng/mL equivalent of rhodomyrtonone. Cells without added compound were used as a negative control. After 24 h incubation, cells were evaluated for viability by MTT assay at a wavelength of 570 nm using a microplate reader (Biohit 830, Biohit, Helsinki, Finland).

Measurement of nitric oxide secretion

The effects of optimized RT-Tr on nitric oxide (NO) secretion were quantified as reported with modification (Syukri et al. 2021). RAW 264.7 cells were plated in 96-well plate at a seeding density of 1×10^4 cells/well. After 24 h incubation, the spent medium was replaced with fresh DMEM containing optimized RT-Tr to yield a final concentration of 3.91–500 ng/mL equivalent rhodomyrtonone. Subsequently, the cells were treated with LPS (50 ng/mL) after an hour to avoid direct interaction. The optical density of supernatant was measured for nitrite level using Grise reagent at 540 nm using a microplate reader (Biohit 830, Biohit, Helsinki, Finland), and nitrile level was quantified in percentage from a standard nitrite curve. Data were expressed as a percentage of nitrite levels relative to the nitrite obtained from cells alone in the LPS-treated cells. Furthermore, the selectivity index (SI) was calculated for transferosome fortified with rhodomyrtonone-rich extract. Moreover, the RAW 264.7 cells obtained from NO quantification were tested for biocompatibility using MTT assay.

Fortification of transferosomes in hydrogel

The optimized RT-Tr formulation was stabilized using Carbopol ultrez-21 as a gelling agent. Briefly, the gel was formulated using 0.5% w/v gelling agent and 0.1% v/v propylene glycol as emollient. Carbopol ultrez-21 (0.5% w/v) was slowly added in the colloidal suspension of optimized vesical entrapped transferosomes fortified with rhodomlyrtone-rich extract with stirring on a magnetic stirrer (SP88857200, Fisher Scientific, USA) followed by addition of propylene glycol and pH regulator triethanolamine. The trapped air bubble was removed by storing overnight in a refrigerator (RT32K5554, Samsung, Thailand) at 4 °C.

Gelling polymer compatibility, physical appearance, viscosity, spreadability, extrudability, and swelling ratio of hydrogel

The functional compatibility of RT-optimized RT-Tr, and RT-Tr stabilized hydrogel was characterized using Fourier Transformed Infrared Spectroscopy (FTIR: BRUKER IFS-66 V, Germany) in an acquisition range of 4000–400 cm^{-1} , with a 4 cm^{-1} resolution. The physical appearance and homogeneity were monitored visually by the naked eye. The viscosity was quantified using a Brookfield viscometer (Brookfield DV-III, USA) with spindle no 3, at 25 ± 1 °C. Spreadability and extrudability were determined, as reported previously (Singh et al. 2021). Briefly, an excess of hydrogel was compressed between two glass plates, the time required to detach the glass plate from each other under an applied force of 0.784 N was recorded as spreadability force using an equation.

$$\text{Spreadability} = \frac{M \times L}{t}$$

where weight (M) in g is kept over the glass slide to move a distance of 'L' in cm in time 't' (s).

RT-Tr stabilized hydrogel was transferred to a collapsible aluminum tube in appropriate quantity and sealed from one end. A weight of 50 g was applied over the tube opening, the quantity of hydrogel extruded was weighed, and the percentage extrusion was calculated. The hydrogel swelling index

was evaluated as reported previously (Ontong et al. 2023). In brief, warm air-dried hydrogel (500 mg) was placed inside a pour bag. The bag was weighed before (W_i) and after (W_f) immersion in demineralized water at 37 °C. The gel-swelling ratio was calculated using the equation.

$$\text{Swelling index} = \frac{W_f - W_i}{W_i} \times 100$$

Biological activity and cytocompatibility of transferosome incorporated hydrogel

RT-Tr and RT-Tr stabilized hydrogel were tested for the antibacterial zone of inhibition against *S. aureus* and *S. epidermidis* using the well diffusion method. The cytotoxicity of test hydrogel was tested against human keratinocytes cells (HaCaT). Briefly, HaCaT cells were seeded in a 96-well plate at a seeding density of 1×10^4 cells/well and treated with RT-Tr hydrogel diluted with DMEM in the range of 7.8–1000 ng/mL equivalent to rhodomlyrtone. Cells without treatment were considered as a negative control. The cell viability was quantified by MTT assay at a wavelength of 560 nm using a microplate spectrophotometer (Biohit 830, Biohit, Helsinki, Finland) after 24 h of incubation.

Stability study

RT-Tr was tested by freeze–thaw test. Briefly, RT-Tr was stored in the stability chamber at 45 °C for 2 day and the refrigerator at 4 °C for 2 days, for 5 cycles. The samples were collected, and pH, vesicle size, surface charge, entrapment efficiency, antimicrobial activity, radical scavenging efficacy, and tyrosinase inhibition efficacy were measured.

Statistical analysis





All experiments were performed in triplicate, and results were presented as mean \pm SD. One-way ANOVA followed by Dunnett's test was used to analyze the significance difference using GraphPad, Version 8 (GraphPad Software Inc., La Jolla, CA, USA). A significant difference was considered as $p < 0.05$.

Table 2 The stability, physical appearance, particle size, zeta potential, and entrapment efficiency of transferosomes

| Formulation code | Physical property | Size (nm) | Zeta (mV) | PDI | Stability test | % EE | Conc. ($\mu\text{g/mL}$) |
|------------------|-------------------------|-----------------|-------------------|-----------------|----------------|------------------|----------------------------|
| Tr-5 | Dark brown-green cloudy | 457.5 ± 3.6 | -44.79 ± 0.76 | 0.33 ± 0.02 | Stable | 37.52 ± 2.56 | 75.50 ± 0.16 |
| Tr-10 | Yellowish green turbid | 419.2 ± 2.6 | -31.15 ± 1.46 | 0.13 ± 0.01 | Stable | 47.77 ± 0.10 | 96.29 ± 0.20 |
| Tr-15 | Brown clear | 405.3 ± 2.0 | -61.62 ± 0.86 | 0.16 ± 0.08 | Stable | 81.90 ± 0.31 | 164.84 ± 0.62 |

NT Not tested, Ppt Precipitate, PDI polydispersity index

Table 3 Color responses and corresponding L, a, b, and E values of transferosome formulations

| Formulations | L* | a* | b* | Hue | Chroma | ΔE | BI |
|---|------------------|-------------------|-----------------|------------------|-----------------|------------------|------------------|
|  Control | 19.96 ± 0.07 | -0.53 ± 0.07 | 1.76 ± 0.07 | -0.25 ± 2.72 | 1.84 ± 0.06 | 20.04 ± 0.07 | 7.07 ± 0.52 |
|  Tr-5 | 29.10 ± 0.05 | -1.80 ± 0.01 | 7.20 ± 0.06 | -0.86 ± 0.06 | 7.42 ± 0.05 | 30.03 ± 0.04 | 22.90 ± 0.31 |
|  Tr-10 | 30.09 ± 0.26 | -1.24 ± 0.025 | 9.08 ± 0.01 | -0.64 ± 0.18 | 9.16 ± 0.01 | 31.45 ± 0.02 | 31.74 ± 0.05 |
|  Tr-15 | 18.99 ± 0.25 | 0.78 ± 0.02 | 1.41 ± 0.04 | -0.23 ± 0.13 | 1.61 ± 0.02 | 19.06 ± 0.02 | 10.53 ± 0.15 |

L* lightness, a* redness, b* yellowness, ΔE total color difference, BI browning Index

Results and discussion

Physicochemical characteristics, vesicle sizes, zeta potential, and entrapment efficiency of rhodomlyrtone transferosome

Rhodomyrtus tomentosa leaf extract rich in phloroglucinol demonstrated significant efficacy against potential pathogens and is considered as novel antibiotic. Moreover, several studies indicated the excellent efficacy of rhodomlyrtone against gram positive pathogen makes it a potential candidate as therapeutic agents against SSTIs. The results of physicochemical properties, color analysis, vesicle size, ZP, and EE (%) of fabricated transferosome vesicles formulations were presented in Table 2 and S2. RT-Tr displayed yellowish brown to dark brown with suitable physical properties prepared using tween 20, tween 80, span 20, span 80, and sodium deoxycholate as edge activator, whereas the formulation containing tween 20, tween 80, span 20, span 80 were precipitated after preparation. The vesicle size of RT-Tr was observed in the

Table 4 pH values before and after thaw test

| Code | pH before thaw test | pH after thaw test |
|---------|---------------------|--------------------|
| RT-Tr5 | 6.46 ± 0.02 | 6.40 ± 0.05 |
| RT-Tr10 | 6.93 ± 0.01 | 7.01 ± 0.02 |
| RT-Tr15 | 7.50 ± 0.01 | 7.41 ± 0.01 |

range of 405–457 nm with a polydispersity index of 0.1–0.3, indicating that the transferosomes were homogeneously dispersed. ZP determination is a significant characterization technique of transferosomes vesicles that estimates the charge, which is employed for understanding the physical stability of the colloidal suspension. The ZP of the RT-Tr was observed in the range of -31 to -61 mV. Encapsulation efficacy was calculated as percentage of rhodomlyrtone entrapped within the RT-Tr. The color analysis displayed light yellowish and dark brownish color for RT-Tr, as presented in Table 3. While pH analysis indicated acidic nature of formulations (Table 4) might be due to the polarity solvent used for extraction. The EE (%) of RT-Tr formulations

ranged from 37.5 to 81.90 of target concentration within vesicles. The RT-Tr vesicles containing lipid in the ratio of 0.74:0.092 (% w/v) with SDS (1% w/v) demonstrated the highest EE (%). The entrapment efficiency of hydrophobic drugs depends on several factors, including the fabrication techniques, geometry of vesicles, lipid concentration, physico-chemical properties of the incorporated compound, possible lipid-drug interactions, and composition of colloidal suspensions (Abd EI Azim et al. 2015). Based on EE (%), RT-transferosome vesicles RT-Tr15 was considered as optimized and target formulations for further assessments. The morphology of the vesicles was further evaluated by SEM, indicating the vesicular characteristics shape (Fig. 2). The morphological results of phosphatidylcholine fortified rhodomlyrtone-rich extract transferosomes vesicles using SEM demonstrated spherical in shape with a relatively monodispersed size distribution.

Antimicrobial activity, antioxidant efficacy, and quantitative phytoconstituents analysis

Rhodomyrtus tomentosa is a medicinal plant with vast phytochemical diversity and pharmacological activity (Ozioma et al. 2022). Minimal inhibitory concentration (MIC) and minimum bactericidal concentration (MBC) of RT-Tr against *S. aureus* and *S. epidermidis* ranged from 8–128 and 64–1024 $\mu\text{g/mL}$, and 8–256 and 64–1024 $\mu\text{g/mL}$, respectively (Table 5). A previous study indicated MIC of 31.25 $\mu\text{g/mL}$ and 32–512 $\mu\text{g/mL}$ against free *R. tomentosa* ethanolic leaf extract against *S. aureus* and *S. epidermidis*, respectively (Ozioma et al. 2022). *Rhodomyrtus tomentosa* leaf extract exert antibacterial activity by disruption of cytoplasmic membrane with induced cell lysis or cell membrane (Limsuwan et al. 2012). Another study indicated that the pure rhodomlyrtone isolated from *R. tomentosa* caused abnormalities at both the cell wall and membrane (Sianglum et al.

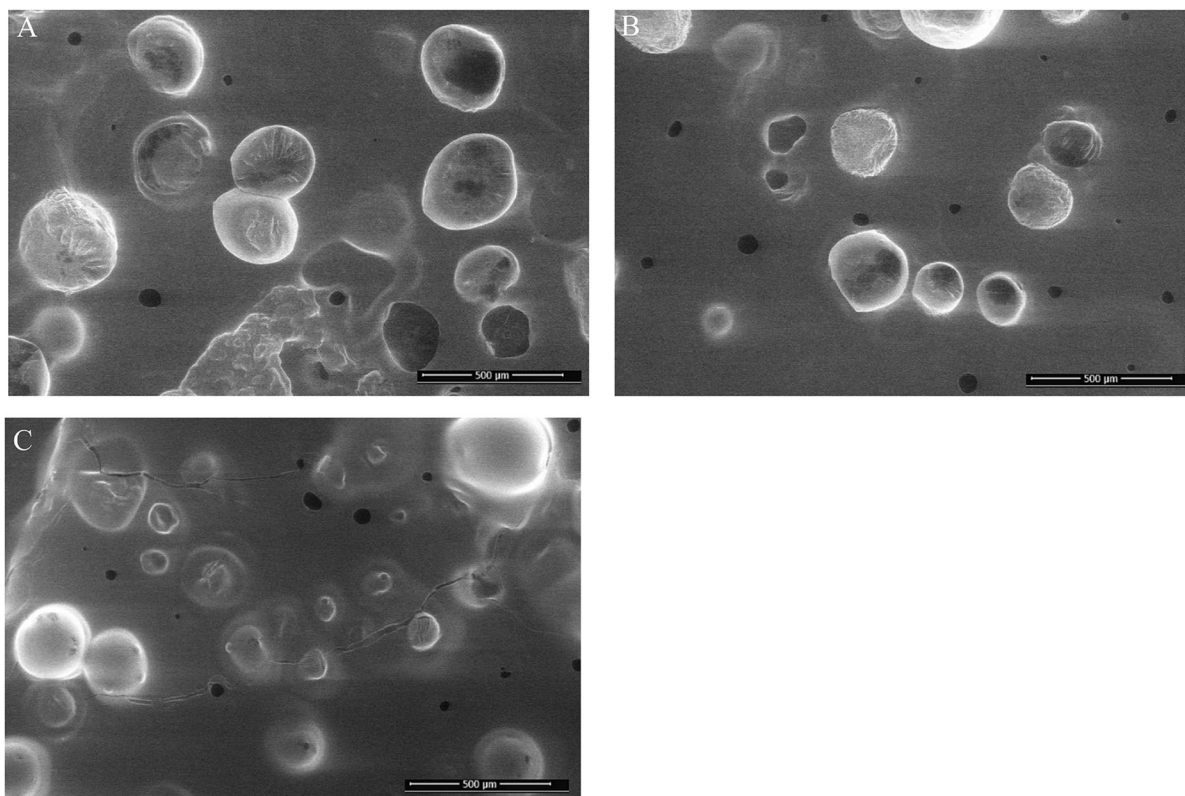


Fig. 2 The morphology of phosphatidylcholine fortified rhodomlyrtone-rich extract transferosomes vesicles RT-Tr5 (A), RT-Tr10 (B), RT-Tr15 (C) using scanning electron microscopy

Table 5 Minimal inhibitory concentration (MIC) and minimum bactericidal concentration (MBC) of RT-transfersomes against *Staphylococcus aureus* ATCC 25923 and *Staphylococcus epidermidis* ATCC 35984*RT Rhodomyrtus tomentosa* leaf, *NT* Not tested

| Code | MIC/MBC ($\mu\text{g}/\text{mL}$) | | | |
|------------|-------------------------------------|-----------------|-----------------------------------|-----------------|
| | <i>Staphylococcus aureus</i> | | <i>Staphylococcus epidermidis</i> | |
| | Before thaw test | After thaw test | Before thaw test | After thaw test |
| RT | 32/64 | NT | 32/64 | NT |
| RT-Tr5 | 128/1024 | 128/1024 | 256/1024 | 256/1024 |
| RT-Tr10 | 64/512 | 64/512 | 64/512 | 64/512 |
| RT-Tr15 | 8/64 | 8/64 | 8/64 | 8/64 |
| Vancomycin | 0.5/0.5 | NT | 0.5/1 | NT |

2011, 2012) with competitively binding to the bacterial cell division protein and inhibitory constant FtsZ (Chorachoo et al. 2015; Saeloh et al. 2017). This result indicated improvement in antimicrobial activity after fortification with lipid-based vesicles due to partition coefficient of lipids within the membrane.

Antioxidants play an important role in regulating reactive radical species by modulating intracellular oxidative stress. Polyphenols are considered potential adjuvant therapy for the scavenging of free radicals. The *in vitro* antioxidant properties of the phenolic-rich RT-Tr demonstrated inhibitory activities against the stable free radical molecules DPPH and ABTS with an IC_{50} of 59.94 ± 2.01 and 148.13 ± 1.01 $\mu\text{g}/\text{mL}$, respectively (Table 6). Total phenolic and flavonoid contents of RT-Tr yielded 15.65 ± 0.04 μg GAE/g extract and 43.13 ± 0.91 μg QE/g extract, respectively. However, RT demonstrated DPPH and ABTS radical scavenging with IC_{50} of 7.79 ± 0.03 and 4.03 ± 0.02 $\mu\text{g}/\text{mL}$, respectively (Idris et al. 2022). Moreover, RT indicated 191.97 ± 0.19 mg GAE/g extract and 29.11 ± 0.05 mg QE/g extract of TPC and TFC, respectively (Idris et al. 2022). The change in potency of radical scavenging is attributed to the

incorporation of target concentration and entrapment of therapeutic agent within vesicles. The antioxidant potential of transfersome vesicles agrees with FTIR spectral analysis, indicating the abundance of hydroxyl groups that can donate electrons or hydrogen to radicals (Olatunde et al. 2019).

Mushroom tyrosinase inhibition assay

Abnormal melanogenesis results in excessive melanin production, leading to pigmentation disorders development. As a key and rate-limiting enzyme for melanogenesis, mushroom tyrosinase has been considered an important target in developing dosage forms against pigment disorder. The results of the tyrosinase inhibition assay indicates that RT-Tr15 displayed moderate activity against mushroom tyrosinase enzyme, with IC_{50} values of 245.32 ± 1.32 $\mu\text{g}/\text{mL}$, compared with standard ascorbic acid (IC_{50} : 112.38 ± 1.23 $\mu\text{g}/\text{mL}$). This result indicates the presence of multiple hydroxyl groups within vesicle-entrapped rhodomyrtone-rich extract, a revisor of natural phenolic compounds responsible for anti-melanogenesis efficacy. Moreover, the position, number,

Table 6 Antioxidant profile of RT 15-transfersomes formulation

| Analysis | RT-Tr15 | | Ascorbic acid | Quercetin |
|---|-------------------|-------------------|-------------------|-----------------|
| | Before thaw test | After thaw test | | |
| DPPH IC_{50} ($\mu\text{g}/\text{mL}$) | 57.94 ± 2.01 | 56.30 ± 2.51 | NA | 8.94 ± 1.35 |
| ABTS IC_{50} ($\mu\text{g}/\text{mL}$) | 148.13 ± 1.01 | 200.93 ± 0.39 | 3.85 ± 0.44 | NA |
| Total phenolic content (μg GAE/g extract) | 15.65 ± 0.04 | 12.50 ± 0.01 | NA | NA |
| Total flavonoid content (μg QE/g extract) | 43.13 ± 0.91 | 34.83 ± 0.36 | NA | NA |
| Tyrosinase inhibitory activities | 245.32 ± 1.32 | 340.72 ± 1.70 | 112.38 ± 1.23 | NA |

DPPH 2,2-diphenyl-1-picrylhydrazyl, *ABTS* 2,2'-azino-bis (3-ethylbenzthiazoline-6-sulphonic acid), *GAE* gallic acid equivalent, *QE* quercetin equivalents, IC_{50} 50% inhibitory concentration, *RT-15* transfersomes formulation, *NA* not applicable

and presences of hydroxyl group with sugar moieties are generally related to tyrosinase inhibition efficacy (Lu et al. 2019). The inhibition of tyrosinase is important in preventing melanin accumulation, especially in facial skin. Therefore, vesicular entrapped tyrosinase inhibitors are an attractive target in the development of cosmetics for treating pigment disorders.

Cytocompatibility of transferosome

Cell culture assay assess the biocompatibility of drug incorporated in the delivery system using isolated cells in vitro. Moreover, these techniques are useful in evaluating the toxicity or irritancy potential of materials or chemicals tested. Thus, the biocompatibility of test RT-TR15 transferosomes was tested against L929 cells, Vero cells, and RAW 264.7 cells to ensure the safety and efficacy of end users. The results of the mitochondrial MTT assay displayed cytotoxicity on L929 cells, Vero cells, and RAW 264.7 with IC_{50} of 7.05 ± 0.17 $\mu\text{g/mL}$, 4.73 ± 0.13 $\mu\text{g/mL}$, and 3.95 ± 0.11 $\mu\text{g/mL}$, respectively (Table 7). The results demonstrated that the RT-Tr15 vesicles were less toxic to L929 cells than Vero cells, equivalent to a 20-fold higher selectivity, compared to doxorubicin. In previous report, the ethanol extract against L929 cell and Vero cell showed IC_{50} of 476 $\mu\text{g/mL}$ (Saising et al. 2012) and 44.87 $\mu\text{g/mL}$, (Marwati et al. 2021) respectively, whereas slight toxic at 50 $\mu\text{g/mL}$ against macrophage cells. In addition, pure rhodomertone displayed the IC_{50} of 200 $\mu\text{g/mL}$ against L929 (Saising et al. 2012), while macrophage showed a viability of ~80% at 2 $\mu\text{g/mL}$. Moreover, microwave-assisted extract exhibited >86% of viability against RAW 264.7 cells concentration ranging from 50–600 ng/mL (Ontong et al. 2023). Furthermore, zebra fish

model, ~80% survival of embryos was demonstrated when treated with pure rhodomertone at 0.5 $\mu\text{g/mL}$ (Siriyoung et al. 2020). Although RT-Tr15 demonstrated biocompatibility in a dose-dependent manner against tested cells, the results suggested that rhodomertone-rich extract-fortified transferosome vesicles were more toxic than previous report due to their rich in rhodomertone content. In previous study with or without microwave assisted *Rhodomertone tomentosa* leaf extract fortified topical gel was tested for safety on human volunteers, the results of hematological and biochemical analysis suggested the formulation was safe at tested concentration (Ontong et al. 2023). Hence, the lipid fortified RT-Tr15 within gel can be effectively employed for the management of skin and soft-tissue infections.

Measurement of nitric oxide secretion

The effect of nitric oxide secretion and RAW 264.7 cell viability in the presence of LPS (50 ng/mL) is presented in Fig. 3. Natural phloroglucinol has shown significant anti-inflammatory activity in various in vitro and in vivo reports. Several studies successfully indicated the anti-inflammatory and immunomodulatory efficacy of rhodomertone and phenolic-rich *R. tomentosa* leaf extract (Jeong et al. 2012; Lavanya et al. 2012). The ability to rhodomertone to modulate the expression of several pro-inflammatory cytokines, including prostaglandin (PG), cyclooxygenase (Pepperberg et al. 2000), inducible NO synthase (iNOS), interleukin-1 (IL-1), interleukin-6 (IL-6), interleukin-12 (IL-12), interleukin-18 (IL-18), tumor necrosis factor-alpha (TNF- α), nuclear factor-kB (NF-kB), extracellular signal-related kinase (Järvinen et al. 2021), toll-like receptor (TLR), mitogen-activated protein kinase (MAPK), spleen tyrosine kinase (Syk and Src), interleukin-associated kinase (IRAK1), interleukin-4 associated kinase (IRAK4) (Jeong et al. 2013), in addition to their antioxidant and reactive oxygen scavenging efficacy (Lavanya et al. 2012) are well documented. Therefore, rhodomertone-rich extract incorporated transferosome vesicles at 3.9 500 ng/mL were further tested for anti-inflammatory efficacy on LPS (50 ng/mL) stimulated macrophages. Alone treatment of cells with LPS was considered a positive control, and cell alone was tested as negative control. The results of NO displayed a dose-dependent reduction of NO

Table 7 Minimum inhibitory concentration (IC_{50}) of RT-Tr15 or doxorubicin against murine mouse fibroblast cell line (L929), African green monkey epithelial kidney cell (Vero), and mouse macrophage cells (RAW 264.7) determined by MTT assays after 24 h treatment

| Cells | IC_{50} ($\mu\text{g/mL}$) | |
|-----------|--------------------------------|-----------------|
| | RT-Tr15 | Doxorubicin |
| Vero | 4.73 ± 0.13 | 2.38 ± 0.15 |
| L929 | 7.05 ± 0.17 | 0.35 ± 0.03 |
| RAW 264.7 | 3.95 ± 0.11 | – |

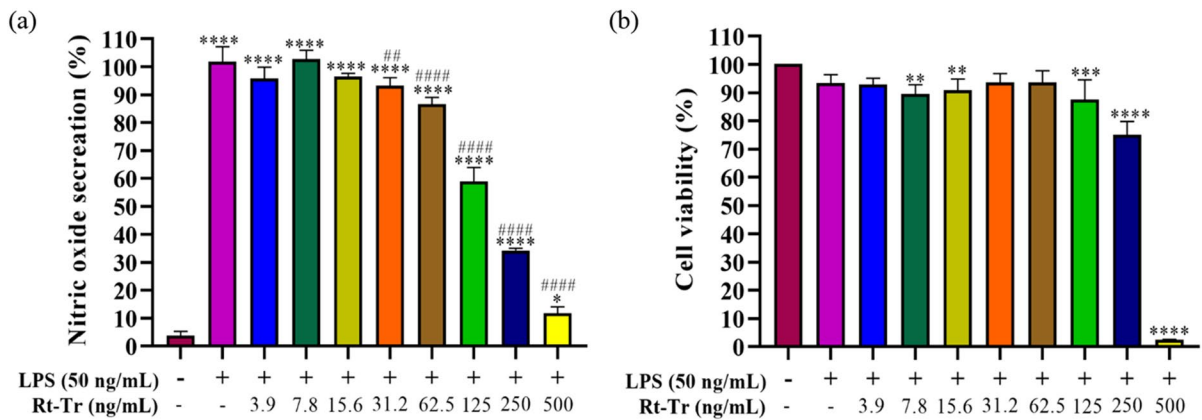


Fig. 3 Nitric oxide secretion was detected by the Griess reagent after stimulation with lipopolysaccharides (50 ng/mL) and with RT-Tr15. Data are presented as mean \pm SEM of two independent experiments performed in triplicate. ## p < 0.05, #### p < 0.001 vs. cell alone; * p < 0.05, **** p < 0.001 vs. the

lipopolysaccharides stimulated group. The combined effect of RT-Tr15 with lipopolysaccharides on RAW 264.7 cells viability using MTT assay. ** p < 0.05, *** p < 0.01, **** p < 0.001 vs. cell alone

secretion. A previous study on rhodomyltone-rich microwave extract demonstrated significant concentration-dependent downregulation of LPS-induced IL-6, IL-1B, iNOS, and COX-2 mRNA (Ontong et al. 2023). Thus, the results suggest that the RT-Tr15 can be considered as a potential candidate for mitigation of SSTIs.

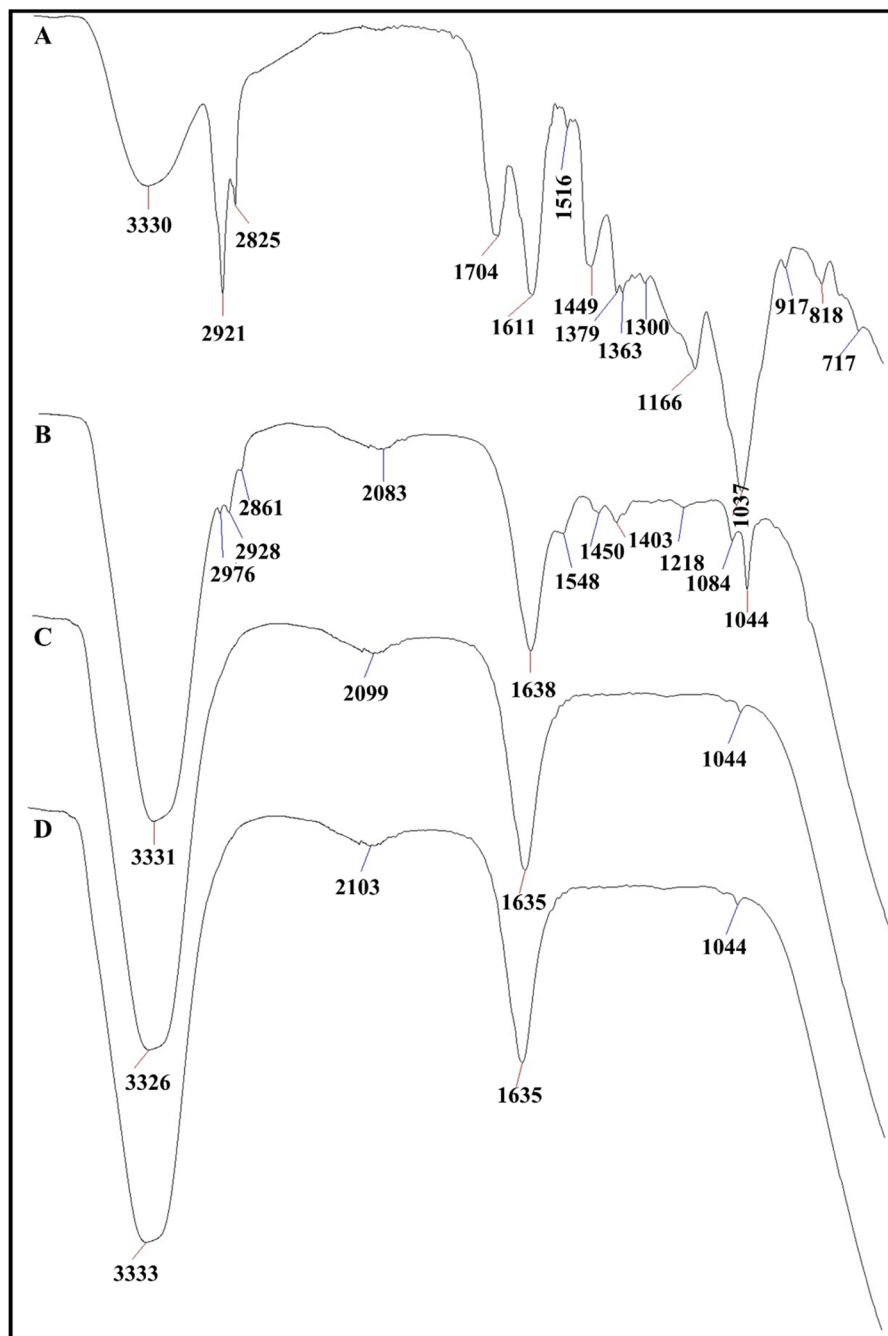
Gelling polymer compatibility, physical appearance, viscosity, spreadability, extrudability, and swelling ratio of hydrogel

Rhodomyltone-rich extract from *R. tomentosa* leaf, RT-Te15 vesicle incorporated bioactive, and stabilized with hydrogel were characterized by ATIR-FTIR spectroscopy (Fig. 4). The RT is a complex mixture of various phytoconstituents, which can be easily seen from FTIR spectrum where some absorption peaks were present. The broadband ~ 3300 cm^{-1} is assigned to intermolecular bounded OH stretching of alcohol, intermolecular bonded weak OH stretching of alcohol attributed to ~ 2900 cm^{-1} , and NH stretching corresponds to ~ 2800 cm^{-1} . The absorption ranges from 2000 to 1650 cm^{-1} ascribed to CH bending, ~ 1550 cm^{-1} assigned for NO stretching, and CH bending corresponds to ~ 1450 cm^{-1} . Moreover, FTIR spectra ranging from 1400–1330 cm^{-1} , 1200–1050 cm^{-1} , and 800–717 cm^{-1} are attributed to OH bending, CO stretching, and CC bending,

respectively. No significant shift in the absorption band was observed for extract and extract-fortified transferosomes. However, a slight change of 3330 cm^{-1} , 2921 cm^{-1} , and 2852 cm^{-1} to 3341 cm^{-1} , 2976 cm^{-1} , and 2861 cm^{-1} , respectively indicated intermolecular bonding between phosphatidylcholine and extract. The polarity of propylene glycol was reflected as improved hydrogen bonding ~ 1440 cm^{-1} (Ontong et al. 2023). The shift and disappearance of major peaks of significant peaks of rhodomyltone-rich extract entrapped in vesicles stabilized within hydrogel were observed due to the dipole interaction between the polar groups of sialic acid and the hydrophobic acyl chains that would restrict the symmetric and asymmetric stretching vibration of CH_2 groups within gelling polymer (Chen and Chiang 2020). The FTIR spectra indicate no chemical interactions between extract and extract incorporated within the vesicle within the stabilized hydrogel.

The results of physical appearance showed that the gel base was transparent. However, the fortification of RT in the vesicles-stabilized hydrogel was dark green. The test and control gel pH were 6.8 and 7.2, respectively. The result of rheology was recorded using a Brookfield viscometer, indicating a significant reduction in the viscosity of test gel compared with control gel base due to pseudoplastic behavior of formulations. Moreover, a decrease in the viscosity of test formulation was attributed

Fig. 4 Vibrational intensity and structural analysis of RT (A), RT-Tr15 transferrin (B), RT-Tr15 transferrin stabilized hydrogel (C), and control gel base (D) using ATR-FTIR in the spectral region range between 4000 – 650 cm^{-1}



to the non-Newtonian behavior of formulations that altered with shear stress (Ontong et al. 2020). The rheological property of hydrogel affects the extrusion and spreadability of formulation from the squeeze tube, which is an important criterion during formulation application and patient acceptance. Moreover, the spreadability of gel differs

due to the presence of bioactive components, polymer concentration, chain length, polydispersity, and proportion of pH regulator. RT-Tr15 stabilized hydrogel and control gel base showed a spread time of 10.2 ± 0.16 s and 14.6 ± 38 s, respectively. While the percentage extrudability was observed 20.06 ± 0.21 and 24.29 ± 0.48 for test and control

gel, respectively, indicating that the concentration of gelling polymer in formulation had adequate consistency. In addition, the results of the swelling ratio of RT-Tr15 stabilized gel ($170.17 \pm 19.0\%$) demonstrated a slight reduction compared to the control gel base ($198.19 \pm 16.1\%$).

Biological activity and cytocompatibility of transferosome incorporated hydrogel

Gram-positive *S. aureus* and *S. epidermidis* are important microorganisms located on human skin and mucosal surface with ability of causing nosocomial infections due to wide usage of medicated topical products representative strain to confirm the antimicrobial efficacy of transferosomes were retained with stabilized hydrogel. The results of the antimicrobial zone of inhibition are presented in Table 8 and Fig. S3. The test and control transferosome stabilized hydrogel showed antimicrobial with a zone of inhibition of 19.25 ± 0.64 (mm) and 17.87 ± 0.62 (mm) against *S. aureus* and *S. epidermidis*, respectively. The gel base fortified with standard vancomycin exhibited a zone of inhibition of 15.16 ± 0.7 (mm) and 12.83 ± 0.28 (mm). In contrast, gel base alone did not show a zone of inhibition against *S. aureus* and *S. epidermidis*, respectively. These results indicated the superior effect of vesicle incorporated rhodomyltone-rich extract. Furthermore, the test and control gel base cytocompatibility was investigated against HaCaT cells at 7.8–1000 ng/mL. The results of the MTT assay indicated ~99.9% of HaCaT cell viability at 250 ng/mL (Fig. 5). This result corroborated with previous rhodomyltone-rich microwave-assisted R.

Table 8 Zone inhibition of formulations against (A) *Staphylococcus aureus* ATCC 25923 and (B) *S. epidermidis* ATCC 12228

| Formulation | Zone inhibition (mm) | |
|---------------------|------------------------------|-----------------------------------|
| | <i>Staphylococcus aureus</i> | <i>Staphylococcus epidermidis</i> |
| Gel with RT-Tr15 | 19.25 ± 0.64 | 17.87 ± 0.62 |
| Gel with Vancomycin | 15.16 ± 0.76 | 12.83 ± 0.28 |
| Control gel base | NA | NA |

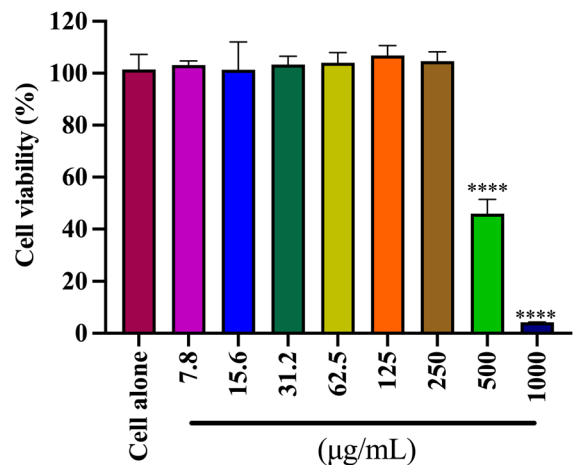


Fig. 5 Biocompatibility of phosphatidylcholine fortified rhodomyltone-rich extract transferosomes vesicles against human keratinocyte cells (HaCaT) at 7.8–1000 ng/mL. **** $p < 0.001$ vs. cell alone

tomentosa extract-incorporated topical gel-treated HaCaT cells (Ontong et al. 2023).

Stability study

An important requirement for the effective use of transferosomes vesicles is the demonstration of controlled size, ZP, and performance stability in the final dosage form. The freeze-thawed stability study results suggested maintained pH, vesicle size, zeta potential, EE (%), antimicrobial activity, radical scavenging efficacy, and tyrosinase inhibition efficacy of RT-transferosomes with no sedimentation (Tables 4, 5, and 6). Moreover, the result indicated that the RT-transferosomes stabilized hydrogel retained the physical property after storage for 30 days at 4 °C.

Conclusion

Phosphatidylcholine blend with cholesterol and sodium deoxycholate fortified rhodomyltone-rich extract from *Rhodomyltus tomentosa* leaf transferosomes vesicles demonstrated improved anti-inflammatory and antimicrobial activity. Rhodomyltone-rich extract incorporated vesicles stabilized with hydrogel showed good physical and antimicrobial activity with significant hydrogen bonding between the vesicle and gelling agent. The anti-inflammatory

activity and cytocompatibility supports the excellent bioactive property of rhodomlyrtone-rich extract as an effective agent in managing skin and soft tissue infections.

Author contributions JCO and SS: Conceptualization, method, investigation, writing-original, review, and editing. TS: Formal analysis. SPV: Conceptualization, funding acquisition, review, and editing.

Funding This work was funded by the National Research Council of Thailand [N41A640071] and partially supported by National Higher Education, Science, Research and Innovation Policy Council, Thaksin University (research project grant) Fiscal Year 2022.

Data availability The data and the materials are all available in this article.

Declarations

Conflict of interest The authors declare no competing interests.

References

- Abd El Azim H, Nafee N, Ramadan A, Khalafallah N (2015) Liposomal buccal mucoadhesive film for improved delivery and permeation of water-soluble vitamins. *Int J Pharm* 488:78–85. <https://doi.org/10.1016/j.ijpharm.2015.04.052>
- Auberon F, Olatunji OJ, Waffo-Teguo P, Olatunde OO, Singh S, Bonté F, Mérillon JM, Lobstein A (2023) Arundinoids I-IX and graminifoliosides AB: 2R-benzylmalate and 2R-isobutylmalates derivatives from *Arundina graminifolia* (D. Don) Hochr. with antioxidant, cytocompatibility and cytoprotective properties. *Phytochem* 206:113504. <https://doi.org/10.1016/j.phytochem.2022.113504>
- Chen M-H, Chiang B-H (2020) Modification of curcumin-loaded liposome with edible compounds to enhance ability of crossing blood brain barrier. *Colloids Surf A* 599:124862. <https://doi.org/10.1016/j.colsurfa.2020.124862>
- Chittasupho C, Chaobankrang K, Sarawungkad A, Samee W, Singh S, Hemsuwimon K, Okonogi S, Kheawfu K, Kiattisinsin K, Chaiyana W (2023) Antioxidant, anti-inflammatory and attenuating intracellular reactive oxygen species activities of *Nicotiana tabacum* var. Virginia leaf extract phytosomes and shape memory gel formulation. *Gels* 9(2):78. <https://doi.org/10.3390/gels9020078>
- Chorachoo J, Amnuakit T, Voravuthikunchai SP (2013) Liposomal encapsulated Rhodomlyrtone: a novel antiacne drug. *Evid Based Complement Altern Med* 2013:157635. <https://doi.org/10.1155/2013/157635>
- Chorachoo J, Saeloh D, Srichana T, Amnuakit T, Musthafa KS, Sretrirutchai S, Voravuthikunchai SP (2016) Rhodomlyrtone as a potential anti-proliferative and apoptosis inducing agent in HaCaT keratinocyte cells. *Eur J Pharmacol* 772:144–151. <https://doi.org/10.1016/j.ejphar.2015.12.005>
- Chorachoo J, Lambert S, Furnholm T, Roberts L, Reingold L, Auepemkiate S, Voravuthikunchai SP, Johnston A (2018) The small molecule rhodomlyrtone suppresses TNF- α and IL-17A-induced keratinocyte inflammatory responses: a potential new therapeutic for psoriasis. *PLoS ONE* 13:e0205340. <https://doi.org/10.1371/journal.pone.0205340>
- CLSI C (2016) Performance standards for antimicrobial susceptibility testing. *Clin Lab Stand Inst* 35:16–38
- Cupane L, Pugacova N, Berzina D, Cauce V, Gardovska D, Miklaševics E (2012) Patients with Panton-Valentine leukocidin positive *Staphylococcus aureus* infections run an increased risk of longer hospitalisation. *Int J Mol Epidemiol Genet* 3:48
- Geetha K, Sridhar C, Murugan V (2010) Antioxidant and healing effect of aqueous alcoholic extract of *Rhodomlyrtus tomentosa* (Ait.) Hassk on chronic gastric ulcers in rats. *J Pharm Res* 3:2860–2862
- Idris M, Sukandar ER, Purnomo AS, Martak F, Fatmawati S (2022) Antidiabetic, cytotoxic and antioxidant activities of *Rhodomlyrtus tomentosa* leaf extracts. *RSC Adv* 12:25697–25710. <https://doi.org/10.1039/D2RA03944C>
- Järvinen E, Deng F, Kiander W, Sinokki A, Kidron H, Sjöstedt N (2022) The role of uptake and efflux transporters in the disposition of glucuronide and sulfate conjugates. *Front Pharmacol* 12:802539–802539. <https://doi.org/10.3389/fphar.2021.802539>
- Jeong D, Yang WS, Yang Y, Nam G, Kim JH, Yoon DH, Noh HJ, Lee S, Kim TW, Sung G-H, Cho JY (2013) *In vitro* and *in vivo* anti-inflammatory effect of *Rhodomlyrtus tomentosa* methanol extract. *J Ethnopharmacol* 146:205–213. <https://doi.org/10.1016/j.jep.2012.12.034>
- Kapoor DU, Gaur M, Parihar A, Prajapati BG, Singh S, Patel RJ (2023) Phosphatidylcholine (PCL) fortified nano-phytopharmaceuticals for improvement of therapeutic efficacy. *EXCLI J* 22:880–903
- Kwiecinski J, Kahlmeter G, Jin T (2015) Biofilm formation by *Staphylococcus aureus* isolates from skin and soft tissue infections. *Curr Microbiol* 70:698–703
- Lavanya G, Voravuthikunchai SP, Towatana NH (2012) Acetone extract from *Rhodomlyrtus tomentosa*: a potent natural antioxidant. *Evid Based Complement Altern Med*. <https://doi.org/10.1155/2012/535479>
- Lei M, Wang L, Olatunde OO, Singh S, Ovatlarnporn C, Basit A, Olatunji OJ (2023) UPLC–ESI–QTOF–MS profiling, antioxidant, antidiabetic, antibacterial, anti-inflammatory, antiproliferative activities and *in silico* molecular docking analysis of *Barleria strigosa*. *Chem Biol Tech Agri* 10(1):73. <https://doi.org/10.1186/s40538-023-00451-2>
- Limsuwan S, Kayser O, Voravuthikunchai SP (2012) Antibacterial activity of *Rhodomlyrtus tomentosa* (Aiton) Hassk. leaf extract against clinical isolates of *Streptococcus pyogenes*. *Evid Based Complement Altern Med* 2012:697183. <https://doi.org/10.1155/2012/697183>
- Lu B, Huang Y, Chen Z, Ye J, Xu H, Chen W, Long X (2019) Niosomal nanocarriers for enhanced skin delivery of quercetin with functions of anti-tyrosinase and antioxidant. *Molecules* 24:2322. <https://doi.org/10.3390/molecules24122322>

- Marwati AAM, Burhan A, Awaluddin A, Nur S, Dharmayanti R, Lilingan E, Tiboyong MD (2021) Antioxidant activity and cytotoxicity against WiDR cell and vero cell of the karamunting (*Rhomyrtus tomentosa* L) leaves ethanol extract. *Indones J Pharam Sci Technol* 8:111–117
- Mordmuang A, Shankar S, Chethanond U, Voravuthikunchai SP (2015) Effects of *Rhomyrtus tomentosa* leaf extract on staphylococcal adhesion and invasion in bovine udder epidermal tissue model. *Nutrients* 7:8503–8517. <https://doi.org/10.3390/nu7105410>
- Mordmuang A, Goodla L, Voravuthikunchai SP (2021) Safety evaluation of *Rhomyrtus tomentosa* leaf extract: sub-acute toxicity assessment in a murine model. *J Complement Med Res* 12:66–75. <https://doi.org/10.5455/jcmr.2021.12.02.10>
- Nagime PV, Singh S, Shaikh NM, Gomare KS, Chitme H, Abdel-Wahab BA, Alqahtany YS, Khateeb MM, Habeeb MS, Bakir MB (2023) Biogenic fabrication of silver nanoparticles using *Calotropis procera* flower extract with enhanced biomimetics attributes. *Materials* 16(11):4058. <https://doi.org/10.3390/ma16114058>
- Nwabor OF, Leejae S, Voravuthikunchai SP (2021a) Rhomyrtone accumulates in bacterial cell wall and cell membrane and inhibits the synthesis of multiple cellular macromolecules in epidemic methicillin-resistant *Staphylococcus aureus*. *Antibiotics* 10:543. <https://doi.org/10.3390/antibiotics10050543>
- Nwabor OF, Singh S, Syukri DM, Voravuthikunchai SP (2021b) Bioactive fractions of *Eucalyptus camaldulensis* inhibit important foodborne pathogens, reduce listeriolysin O-induced haemolysis, and ameliorate hydrogen peroxide-induced oxidative stress on human embryonic colon cells. *Food Chem* 344:128571. <https://doi.org/10.1016/j.foodchem.2020>
- Olatunde OO, Benjakul S, Vongkamjan K, Amnuaitit T (2019) Liposomal encapsulated ethanolic *Coconut husk* extract: antioxidant and antibacterial properties. *J Food Sci* 84:3664–3673. <https://doi.org/10.1111/1750-3841.14853>
- Ontong JC, Singh S, Nwabor OF, Chusri S, Voravuthikunchai SP (2020) Potential of antimicrobial topical gel with synthesized biogenic silver nanoparticle using *Rhomyrtus tomentosa* leaf extract and silk sericin. *Biotechnol Lett* 42:2653–2664. <https://doi.org/10.1007/s10529-020-02971-5>
- Ontong JC, Singh S, Nwabor OF, Chusri S, Kaewnam W, Kanokwiroon K, Septama AW, Panichayupakaranant P, Voravuthikunchai SP (2023) Microwave-assisted extract of rhomyrtone from *Rhomyrtus tomentosa* leaf: anti-inflammatory, antibacterial, antioxidant, and safety assessment of topical rhomyrtone formulation. *Sep Sci Technol* 58:1–15. <https://doi.org/10.1080/01496395.2023.2169162>
- Ozioma FN, Sudarshan S (2022) A Systematic review on *Rhomyrtus tomentosa* (Aiton) Hassk: a potential source of pharmacological relevant bioactive compounds with prospects as alternative remedies in varied medical conditions. *Int J PharmSci Nanotechnol*. <https://doi.org/10.37285/ijpsn.2022.15.2.7>
- Patel R, Singh S, Singh S, Sheth N, Gendle R (2009) Development and characterization of curcumin loaded transferosome for transdermal delivery. *J Pharm Sci Res* 1:71
- Pepperberg IM, Wilcox SE (2000) Evidence for a form of mutual exclusivity during label acquisition by grey parrots (*Psittacus erithacus*). *J Comp Psychol* 114:219–231
- Popat M, Sudarshan S, Anil P, Adinath S, Bhupendra GP (2023) Lipid-based oral formulation in capsules to improve the delivery of poorly water-soluble drugs. *Front Drug Deliv*. <https://doi.org/10.3389/fddev.2023.1232012>
- Saeloh D, Wenzel M, Rungrotmongkol T, Hamoen LW, Tipmanee V, Voravuthikunchai SP (2017) Effects of rhomyrtone on Gram-positive bacterial tubulin homologue FtsZ. *Peer J* 5:e2962
- Saising J, Voravuthikunchai SP (2012) Anti *Propionibacterium acnes* activity of rhomyrtone, an effective compound from *Rhomyrtus tomentosa* (Aiton) Hassk. leaves. *Anaerobe* 18:400–404. <https://doi.org/10.1016/j.anaerobe.2012.05.003>
- Sianglum W, Srimanote P, Wonglumsom W, Kittiniyom K, Voravuthikunchai SP (2011) Proteome analyses of cellular proteins in methicillin-resistant *Staphylococcus aureus* treated with rhomyrtone, a novel antibiotic candidate. *PLoS ONE* 6:e16628. <https://doi.org/10.1371/journal.pone.0016628>
- Sianglum W, Srimanote P, Taylor PW, Rosado H, Voravuthikunchai SP (2012) Transcriptome analysis of responses to rhomyrtone in methicillin-resistant *Staphylococcus aureus*. *PLoS ONE* 7:e45744. <https://doi.org/10.1371/journal.pone.0045744>
- Singh S, Dodiya TR, Singh S, Dodiya R (2021) Topical wound healing, antimicrobial and antioxidant potential of *Mimosa pudica* Linn root extracted using n-hexane followed by methanol, fortified in ointment base. *Int J Pharm Sci Nanotechnol* 14:5472–5480
- Singh S, Chunglok W, Nwabor OF, Chulrik W, Jansakun C, Bhoopong P (2022a) Porous biodegradable sodium alginate composite fortified with *Hibiscus sabdariffa* L. calyx extract for the multifarious biological applications and extension of climacteric fruit shelf-life. *J Polym Environ* 31:922–938. <https://doi.org/10.1007/s10924-022-02596-x>
- Singh S, Chunglok W, Nwabor OF, Ushir YV, Singh S, Panpipat W (2022b) Hydrophilic biopolymer matrix antibacterial peel-off facial mask functionalized with biogenic nanostructured material for cosmeceutical applications. *J Polym Environ* 30:938–953. <https://doi.org/10.1007/s10924-021-02249-5>
- Singh S, Chidrawar VR, Hermawan D, Nwabor OF, Olatunde OO, Jayeoye TJ, Samee W, Ontong JC, Chittasupho C (2023a) Solvent-assisted dechlorophyllization of *Psidium guajava* leaf extract: effects on the polyphenol content, cytocompatibility, antibacterial, anti-inflammatory, and anticancer activities. *South African J Bot* 158:166–179. <https://doi.org/10.1016/j.sajb.2023.04.029>
- Singh S, Chidrawar VR, Hermawan D, Dodiya R, Samee W, Ontong JC, Ushir YV, Prajapati BG, Chittasupho C (2023b) Hypromellose highly swellable composite fortified with *Psidium Guajava* leaf phenolic-rich extract for antioxidative, antibacterial, anti-inflammatory, anti-melanogenesis, and hemostasis applications. *J Polym Environ*. <https://doi.org/10.1007/s10924-023-02819-9>
- Siriyong T, Ontong JC, Leejae S, Suwalak S, Coote PJ, Voravuthikunchai SP (2020) *In vivo* safety assessment of rhomyrtone, a potent compound, from *Rhomyrtus*

- tomentosa* leaf extract. Toxicol Rep 7:919–924. <https://doi.org/10.1016/j.toxrep.2020.07.013>
- Stevens DL, Bisno AL, Chambers HF, Everett ED, Dellinger P, Goldstein EJC, Gorbach SL, Hirschmann JV, Kaplan EL, Montoya JG, Wade JC (2005) Practice guidelines for the diagnosis and management of skin and soft-tissue infections. Arch Clin Infect Dis 41:1373–1406
- Syukri DM, Nwabor OF, Singh S, Voravuthikunchai SP (2021) Antibacterial functionalization of nylon monofilament surgical sutures through in situ deposition of biogenic silver nanoparticles. Surf Coat Technol 413:127090. <https://doi.org/10.1016/j.surfcoat.2021.127090>
- Voravuthikunchai SP, Dolah S, Charernjiratrakul W (2010) Control of *Bacillus cereus* in foods by *Rhodomyrtus tomentosa* (Ait.) hassk. leaf extract and its purified compound. J Food Prot 73:1907–1912. <https://doi.org/10.4315/0362-028X-73.10.1907>
- Wunnoo S, Billman S, Amnuaikit T, Ontong JC, Singh S, Auepemkiate S, Voravuthikunchai SP (2021) Rhodomyrtone as a new natural antibiotic isolated from *Rhodomyrtus tomentosa* leaf extract: a clinical application in the management of acne vulgaris. Antibiotics 10:108. <https://doi.org/10.3390/antibiotics10020108>
- Xavier-Santos JB, Passos JGR, Gomes JAS, Cruz JVC, Alves JSF, Garcia VB, da Silva RM, Lopes NP, Araujo-Junior RF, Zucolotto SM, Silva-Junior AA, Félix-Silva J, Fernandes-Pedrosa MF (2022) Topical gel containing phenolic-rich extract from *Ipomoea pes-capre* leaf (Convolvulaceae) has anti-inflammatory, wound healing, and antiophidic properties. Biomed Pharmacother 149:112921. <https://doi.org/10.1016/j.biopha.2022.112921>

Publisher's Note Springer Nature remains neutral with regard to jurisdictional claims in published maps and institutional affiliations.

Springer Nature or its licensor (e.g. a society or other partner) holds exclusive rights to this article under a publishing agreement with the author(s) or other rightsholder(s); author self-archiving of the accepted manuscript version of this article is solely governed by the terms of such publishing agreement and applicable law.